JACS
JOURNAL OF THE AMERICAN CHEMICAL SOCIETY

Communication

pubs.acs.org/JACS

Colloidal Hybrid Nanoparticle Insertion Reaction for Transforming Heterodimers into Heterotrimers

Carlos G. Read, Thomas R. Gordon, James M. Hodges, and Raymond E. Schaak*

Department of Chemistry and Materials Research Institute, The Pennsylvania State University, University Park, Pennsylvania 16802, United States

Supporting Information

ABSTRACT: Three-component colloidal hybrid nanoparticles, which are central to a diverse array of applications, are typically synthesized using successive seeded growth steps, which are additive in nature and driven by surface chemistry considerations and material-specific preferences for nucleation and growth. Here, we describe a new nanoparticle insertion reaction for transforming heterodimers into heterotrimers, which is based on a supersaturation–precipitation pathway that shifts the driving force for heterotrimer formation away from surface-driven nucleation and growth. To demonstrate the concept, a Ge segment is inserted between the Au and Fe_3O_4 domains of Au–Fe_3O_4 heterodimers to form Au–Ge–Fe_3O_4 heterotrimers. Microscopic investigations reveal important mechanistic insights, including identification of a proposed Au–Ge–Au–Fe_3O_4 intermediate. The process can be modified to access the analogous addition product Ge–Au–Fe_3O_4, allowing tuning between two distinct heterotrimer isomers with different configurations.

Multicomponent colloidal hybrid nanoparticles with precisely defined configurations and interfaces underpin a growing number of applications that include solar energy conversion,[1−3] catalysis,[4−6] photonics,[7] electronics,[8] and theranostics.[9] Most hybrid nanoparticles contain two domains that are connected together through a solid–solid interface, which permits electronic, optical, and magnetic coupling as well as multifunctionality and orthogonal surface derivatization in spatially distinct regions.[10,11] For example, Au–Fe_3O_4 nanoparticle heterodimers exhibit simultaneous plasmonic and magnetic properties and are catalytically active for H_2O_2 reduction,[4] CO oxidation,[5] and nitrophenol reduction.[6] Additionally, their Au and Fe_3O_4 surfaces can be orthogonally functionalized with cisplatin analogues and tumor-specific targeting agents via thiol and diol linkers, respectively, to enable advanced capabilities for cancer therapeutics.[12] While synthetic capabilities and applications for colloidal heterodimers are rapidly expanding, higher-order hybrid nanoparticles such as three-component heterotrimers offer even greater functional diversity.[10,11] For example, trimeric Au–MnO–SiO_2 hybrid nanoparticles incorporate an accessible Au surface for bioconjugation via thiol coupling, a magnetic MnO core for MRI contrast, and a PEG-functionalized, dye-embedded SiO_2 coating on the MnO domain to permit water solubility, biocompatibility, and further bioconjugation via silane coupling.[13] Similarly, overall water splitting can be facilitated by three-component hybrid nanostructures that have a central light-absorbing semiconductor connected to a hydrogen evolving catalyst on one side and an oxygen evolving catalyst on the other.[14]

Colloidal heterotrimers are typically produced through successive seeded growth steps, which inherently are additive in nature and are driven by, and at the same time limited by, surface chemistry considerations and material-specific preferences for nucleation and growth.[15] The reliance on surface-seeded nucleation and growth places constraints on the materials, morphologies, and connectivities that can be accessed, especially for the trimeric systems mentioned above. Here, we report a conceptually new approach for synthesizing trimeric colloidal hybrid nanoparticles, whereby a third nanoparticle domain can be inserted selectively between the two domains of a heterodimer seed. This alternate pathway exploits nanoparticle-mediated supersaturation–precipitation processes, such as solution–liquid–solid (SLS) growth,[16,17] which shifts the driving force for heterotrimer formation away from surface-driven nucleation and growth. The nanoparticle insertion process is demonstrated for the transformation of Au–Fe_3O_4 heterodimers into Au–Ge–Fe_3O_4 heterotrimers. Furthermore, we provide preliminary evidence that the insertion reaction is general and also show that it can be modified to permit tuning between insertion and addition pathways for the same system, selectively producing Au–Ge–Fe_3O_4 vs. Ge–Au–Fe_3O_4 heterotrimer isomers.

Figure 1a shows a TEM image of a representative sample of Au–Fe_3O_4 heterodimers, which were synthesized as reported previously.[18] Each Au–Fe_3O_4 heterodimer consists of a Au nanoparticle connected to a Fe_3O_4 nanoparticle; this assignment is confirmed by the STEM-EDS element map in the inset to Figure 1a. Upon rapid injection of a 1-octadecene solution of Ge(II)bis(hexamethyldisilylamide) [$Ge(HMDS)_2$] into a mixture of 1-octadecene, oleylamine, oleic acid, trioctylphosphine, and the Au–Fe_3O_4 heterodimers at ∼300 °C for 35 min, the product shown in the TEM image in Figure 1b forms. A majority of the particles in Figure 1b appear as trimeric constructs that resemble the Au–Fe_3O_4 heterodimer seeds but with an additional central segment of variable length. Analysis of this and additional TEM images reveals a morphological yield of approximately 80% for the insertion product, along with approximately 20% unreacted or partially reacted Au–Fe_3O_4

Received: August 20, 2015
Published: September 21, 2015

DOI: 10.1021/jacs.5b08850
J. Am. Chem. Soc. 2015, 137, 12514−12517

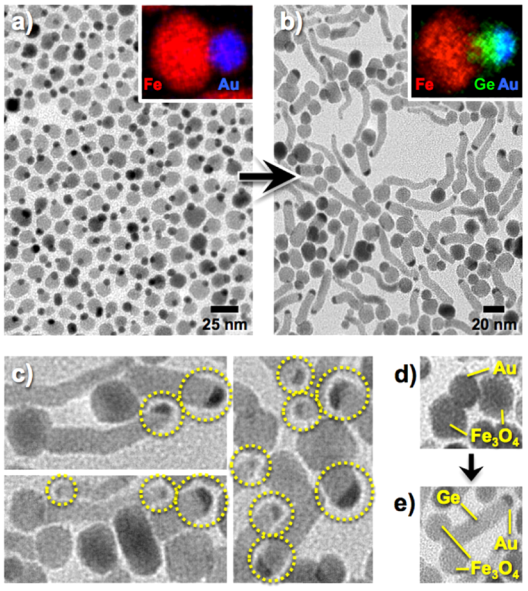

Figure 1. TEM images of (a) Au–Fe_3O_4 heterodimer seeds, (b) Au–Ge–Fe_3O_4 heterotrimer products, and (c) a collection of Au–Ge–Fe_3O_4 heterotrimers with the Au nanoparticle tips highlighted in yellow dashed circles; the size of the Au domain correlates with the thickness of the Ge segment. (d,e) TEM images of a two-lobed Fe_3O_4–Au–Fe_3O_4 seed and the resulting Fe_3O_4–Au(Ge)–Fe_3O_4 hybrid structure. The insets to panels (a) and (b) show STEM-EDS element maps of the corresponding Au–Fe_3O_4 and Au–Ge–Fe_3O_4 particles.

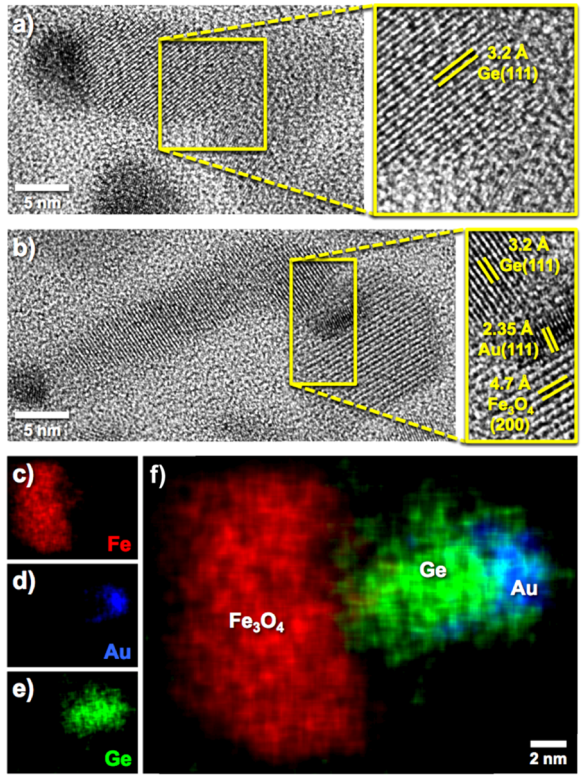

Figure 2. (a,b) HRTEM images of the two types of hybrid nanoparticle products, Au–Ge–Fe_3O_4 and Au–Ge–Au–Fe_3O_4, that result from Ge insertion. (c–f) STEM-EDS element maps of a representative Au–Ge–Fe_3O_4 heterotrimer.

heterodimers. The STEM-EDS element map in the inset of Figure 1b shows the presence of Ge between the Au and Fe_3O_4 domains, suggesting that the Ge inserts between the Au and Fe_3O_4 domains to transform the Au–Fe_3O_4 heterodimers into related Au–Ge–Fe_3O_4 heterotrimers.

The as-synthesized heterotrimers exhibit a combination of bent and straight Ge segments with lengths that range from ~10 nm up to ~55 nm. Furthermore, as shown in Figure 1c, the thicknesses of the Ge domains appear to correlate with the sizes of the gold nanoparticle seeds, which is consistent with previous reports on the Au nanoparticle-seeded growth of Ge nanostructures using supersaturation–precipitation pathways.[16,17] Figure 1d shows a TEM image of a Fe_3O_4–Au–Fe_3O_4 particle, which is a distinct type of hybrid construct that comprises approximately 6% of the Au–Fe_3O_4 heterodimer sample. Upon reaction with $Ge(HMDS)_2$, Ge also inserts into the Fe_3O_4–Au–Fe_3O_4 particle, forming the Fe_3O_4–Au(Ge)–Fe_3O_4 hybrid construct shown in Figure 1e. Retention of the two Fe_3O_4 lobes, with insertion of the Ge at their intersection where the Au had been located, further validates the insertion pathway, rather than an alternate dissolution–reprecipitation process, because the unique morphological characteristics of the seeds remain intact.

Figure 2a,b shows high-resolution TEM images of two representative heterostructures, which highlight the range of insertion products that are observed. Figure 2a shows the predominant morphology, which is a heterotrimer containing a central Ge nanowire segment capped by a Au domain on one end and a Fe_3O_4 domain on the other. As shown in Figure 2b, related Au–Ge–Au–Fe_3O_4 species are also observed, likely produced by the segregation of the Au domain into two distinct nanoparticles, with one Au segment located at the tip and the other remaining at the base of the Ge nanowire and also interfacing with the Fe_3O_4 domain; the formation of this product will be discussed in more detail below. The products in Figure 2a,b contain nanoparticle segments having observed lattice spacings of 3.2, 2.35, and 4.7 Å, which closely match the Ge(111), Au(111), and Fe_3O_4(200) planes, respectively. Additional HRTEM images are shown in Figure S1 in the Supporting Information. STEM-EDS element maps for Fe (Figure 2c), Au (Figure 2d), and Ge (Figure 2e), along with the overlay in Figure 2f, further confirm the presence and configuration of the three distinct nanoparticle domains. The STEM-EDS maps also indicate that small amounts of Au (~10 at. %) are present in the Ge domain, consistent with the proposed supersaturation–precipitation growth mechanism, as discussed below.

Interestingly, the addition of a smaller amount of $Ge(HMDS)_2$ to the Au–Fe_3O_4 heterodimers than was used to produce the Au–Ge–Fe_3O_4 insertion product (e.g., a ~5:1 $Ge(HMDS)_2$ to Au–Fe_3O_4 ratio instead of the ~15:1 ratio that was used previously) instead leads to the formation of an analogous addition product, as seen in the TEM image in Figure 3a. Here, the Ge domain appears to add directly to the preexisting Au nanoparticle domain instead of inserting between the Au and Fe_3O_4 domains, forming a Ge–Au–Fe_3O_4 product that can be considered as a distinct heterotrimer isomer relative to the Au–Ge–Fe_3O_4 insertion product. This indicates that small changes to the reaction conditions can permit tuning between insertion and addition pathways, leading to multiple distinct heterotrimer isomers in the same three-component system. Previous routes to colloidal heterotrimer isomers, which are rare yet important because of the critical roles that domain configurations and interfaces have on the synergistic properties, required the use of a nanoparticle protecting group.[19] The Ge–Au–Fe_3O_4 addition product is obtained in approximately 95% morphological yield,

DOI: 10.1021/jacs.5b08850
J. Am. Chem. Soc. 2015, 137, 12514–12517

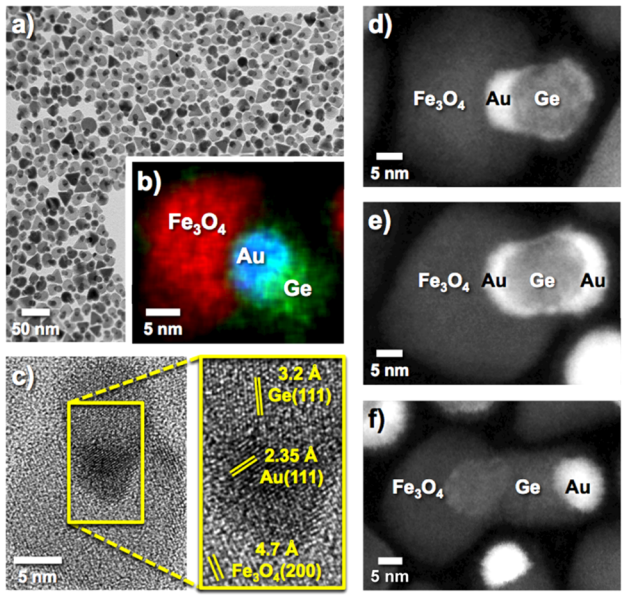

Figure 3. (a) TEM image, (b) STEM-EDS element map, (c) HRTEM image, and (d) HAADF-STEM image of Ge−Au−Fe_3O_4 heterotrimers resulting from Ge addition rather than insertion. HAADF-STEM images showing (e) the proposed Au−Ge−Au−Fe_3O_4 intermediate and (f) the Au−Ge−Fe_3O_4 insertion product.

with approximately 5% of the product consisting of Au−Ge−Fe_3O_4 insertion products and unreacted Au−Fe_3O_4 heterodimer seeds. The STEM-EDS element map in Figure 3b confirms both the presence of the distinct Ge, Au, and Fe_3O_4 domains and their arrangement in a Ge−Au−Fe_3O_4 configuration. The corresponding HRTEM image in Figure 3c shows three nanoparticle domains that are crystalline, with observed lattice spacings of 3.2, 2.35, and 4.7 Å that closely match the Ge(111), Au(111), and Fe_3O_4(200) planes, respectively. The HAADF-STEM image in Figure 3d also clearly shows the Ge−Au−Fe_3O_4 domain sequence.

The HAADF-STEM image in Figure 3e captures a hybrid nanoparticle that contains Ge surrounded by Au in a Au−Ge−Au−Fe_3O_4 configuration, which is a likely intermediate in the formation of the final Au−Ge−Fe_3O_4 insertion product, shown for comparison in Figure 3f. The proposed Au−Ge−Au−Fe_3O_4 intermediate, which was observed frequently, is noteworthy because it shows Ge encapsulated within a shell of Au. This observation suggests that the Ge begins its insertion between the Au−Fe_3O_4 interface by incorporating into, and precipitating within, the Au domain, as is frequently observed in Au-seeded supersaturation−precipitation pathways to Ge nanowires and Au−Ge nanoparticles.[20−22]

To grow Ge and related semiconductor nanowires through solution−liquid−solid (SLS) and vapor−liquid−solid (VLS) supersaturation−precipitation pathways, Au and related seed nanoparticles are often deposited onto surfaces.[20−22] It is well-known that these nanoparticle seeds can either remain bound to the substrate, with the semiconductor nanowire growing outward, or advance along with the tip of the growing semiconductor nanowire. In the latter case, the semiconductor nanowire effectively inserts between the substrate and the substrate-anchored nanoparticle seed. Whether the semiconductor nanowire grows outward from the substrate-anchored seed or inserts between the substrate and the seed depends on the substrate−seed interfacial energy and whether or not the seed and substrate can be separated from one another during the supersaturation−precipitation process.[20−22] We propose, therefore, that as the Ge begins to precipitate from the supersaturated Au−Ge alloy that remains attached to the surface of the Fe_3O_4 domain, the preference is for the Au domain to remain at the tip of the growing Ge nanowire, which ultimately produces the Au−Ge−Fe_3O_4 insertion product. However, at the early stages of the insertion reaction, the stable Au−Fe_3O_4 interface can be retained, and some of the Au remains at that interface. The proposed Au−Ge−Au−Fe_3O_4 intermediate shown in Figure 3e, and also in Figure S2, is therefore consistent with a process whereby maintaining the Au−Fe_3O_4 interface competes with the Au domain advancing with the tip of the growing Ge domain. To fully transform the proposed Au−Ge−Au−Fe_3O_4 intermediates into the complete Au−Ge−Fe_3O_4 insertion products, the Au bound at the buried Au−Fe_3O_4 interface migrates to the Ge surface and ultimately to the Au nanoparticle on the tip of the Ge domain. Consistent with this, some Au is observed by STEM-EDS around the Ge domains, as shown in Figure 2d.

To begin expanding the scope of the nanoparticle insertion reaction, we targeted systems with different domain materials. For example, preliminary evidence, shown in Figure S3, suggests that the Ge insertion reaction also can be applied to Au−In_2O_3 heterodimer seeds,[23] producing Au−Ge−In_2O_3 heterotrimers. In addition, Figure S4 shows a HRTEM image and corresponding STEM-EDS element maps of a Au−FeGe−Fe_3O_4 heterotrimer, providing preliminary evidence that Fe incorporation during the Ge insertion reaction can lead to the formation of alloy domains.

In conclusion, we have demonstrated a new nanoparticle insertion reaction for transforming colloidal heterodimers into higher-order heterotrimers. The process exploits a supersaturation−precipitation pathway originally developed for the growth of semiconductor nanowires. As such, it shifts the driving force for heterotrimer formation away from traditional surface-driven seeded nucleation and growth and therefore opens new doors for the design and synthesis of high-order hybrid nanoparticle constructs that integrate central semiconductor segments with metals and oxides bound at opposite ends. In addition, the ability to tune between addition and insertion pathways provides access to distinct heterotrimer isomers, Ge−Au−Fe_3O_4 vs. Au−Ge−Fe_3O_4, which contain the same materials but with different configurations; such configurational control is challenging to achieve for multicomponent colloidal hybrid nanoparticle systems. Finally, while this initial demonstration focused on a prototype system and characterization of the process by which the insertion reaction occurs, preliminary evidence suggests that it may be general to other metal, alloy, metal oxide, and semiconductor components. Further optimization of reaction conditions will likely lead to narrower product distributions, as well as control over additional morphological features, such as Ge segment lengths.

■ ASSOCIATED CONTENT

Supporting Information

The Supporting Information is available free of charge on the ACS Publications website at DOI: 10.1021/jacs.5b08850.

Experimental details and additional TEM and HRTEM images and STEM-EDS element maps (PDF)

DOI: 10.1021/jacs.5b08850
J. Am. Chem. Soc. 2015, 137, 12514−12517

AUTHOR INFORMATION

Corresponding Author

*res20@psu.edu

Notes

The authors declare no competing financial interest.

ACKNOWLEDGMENTS

This work was supported by the U.S. National Science Foundation under grant CHE-1410061. TEM imaging was performed in the Penn State Microscopy and Cytometry facility, and HRTEM imaging was performed at the Materials Characterization Lab of the Penn State Materials Research Institute. The authors thank Ke Wang for assistance in collecting the TEM images.

REFERENCES

(1) Amirav, L.; Alivisatos, A. P. *J. Phys. Chem. Lett.* **2010**, *1*, 1051−1054.
(2) Costi, R.; Saunders, A. E.; Elmalem, E.; Salant, A.; Banin, U. *Nano Lett.* **2008**, *8*, 637−641.
(3) Khon, E.; Lambright, K.; Khnayzer, R. S.; Moroz, P.; Perera, D.; Butaeva, E.; Lambright, S.; Castellano, F. C.; Zamkov, M. *Nano Lett.* **2013**, *13*, 2016−2023.
(4) Lee, Y.; Garcia, M.; Frey Huls, N. A.; Sun, S. *Angew. Chem., Int. Ed.* **2010**, *49*, 1271−1274.
(5) Wang, C.; Yin, H.; Dai, S.; Sun, S. *Chem. Mater.* **2010**, *22*, 3277−3282.
(6) Lin, F. H.; Doong, R. A. *J. Phys. Chem. C* **2011**, *115*, 6591−6598.
(7) Shaviv, E.; Schubert, O.; Alves-Santos, M.; Goldoni, G.; Felice, D. R.; Vallee, F.; Fatti, N. D.; Banin, U.; Sonnichsen, C. *ACS Nano* **2011**, *5*, 4712−4719.
(8) Mokari, T.; Rothenberg, E.; Popov, I.; Costi, R.; Banin, U. *Science* **2004**, *304*, 1787−1790.
(9) Leung, K. C.-F.; Xuan, S.; Zhu, X.; Wang, D.; Chak, C.-P.; Lee, S.-F.; Ho, W. K.-W.; Chung, B. C.-T. *Chem. Soc. Rev.* **2012**, *41*, 1911−1928.
(10) Buck, M. R.; Schaak, R. E. *Angew. Chem., Int. Ed.* **2013**, *52*, 6154−6178.
(11) Buck, M. R.; Bondi, J. F.; Schaak, R. E. *Nat. Chem.* **2012**, *4*, 37−44.
(12) Xu, C.; Wang, B.; Sun, S. *J. Am. Chem. Soc.* **2009**, *131*, 4216−4217.
(13) Schick, I.; Lorenz, S.; Gehrig, D.; Schilmann, A.-M.; Bauer, H.; Panthöfer, M.; Fischer, K.; Strand, D.; Laquai, F.; Tremel, W. *J. Am. Chem. Soc.* **2014**, *136*, 2473−2483.
(14) Kamat, P. V. *J. Phys. Chem. Lett.* **2012**, *3*, 663−672.
(15) Bradley, M. J.; Read, C. G.; Schaak, R. E. *J. Phys. Chem. C* **2015**, *119*, 8952−8959.
(16) Read, C. G.; Biacchi, A. J.; Schaak, R. E. *Chem. Mater.* **2013**, *25*, 4304−4311.
(17) Hanrath, T.; Korgel, B. A. *J. Am. Chem. Soc.* **2002**, *124*, 1424−1429.
(18) Yu, H.; Chen, M.; Rice, P. M.; Wang, S. X.; White, R.; Sun, S. *Nano Lett.* **2005**, *5*, 379−382.
(19) Hodges, J. M.; Biacchi, A. J.; Schaak, R. E. *ACS Nano* **2014**, *8*, 1047−1056.
(20) Wang, D.; Dai, H. *Angew. Chem., Int. Ed.* **2002**, *41*, 4783−4786.
(21) Wu, Y.; Yang, P. *J. Am. Chem. Soc.* **2001**, *123*, 3165−3166.
(22) Morales, A. M.; Lieber, C. M. *Science* **1998**, *279*, 208−211.
(23) Gordon, T. R.; Schaak, R. E. *Chem. Mater.* **2014**, *26*, 5900−5904.

DOI: 10.1021/jacs.5b08850
J. Am. Chem. Soc. 2015, 137, 12514−12517